

Water dispersible Ag@polyaniline-pectin as supercapacitor electrode for physiological environment†

Cite this: *J. Mater. Chem. B*, 2014, 2, 5012

Chellachamy A. Amarnath,^a Nandakumar Venkatesan,^b Mukesh Doble^b and Shilpa N. Sawant^{*a}

Designing the supercapacitor electrode material for implantable electronic medical devices (IEMDs) requires careful consideration because of the need for materials which are inherently high in capacitance, biocompatibility, and antibacterial activity and are able to work in physiological environment. For the first time, we report the synthesis of a nanocomposite which has the aforementioned properties and demonstrate the nanocomposite as a supercapacitor electrode material operating in physiological fluids. In the first step, water dispersible polyaniline-pectin (PANI-PEC) nanoparticles were synthesized using biopolymer pectin (PEC) as the stabilizer. In the second step, the synthesized PANI-PEC was treated with a silver nitrate solution to afford silver nanoparticles (Ag NPs) decorated PANI-PEC nanocomposite (Ag@PANI-PEC). PANI-PEC acted as a reducing agent to convert silver ions to Ag NPs, thus eliminating the need of an exogenous reducing agent. Ag@PANI-PEC displays a specific capacitance of 140, 290, 144 and 121 F g⁻¹ in phosphate buffer saline, blood, urine and serum, respectively, which are all physiological fluids. Furthermore, due to the use of biopolymer PEC, PANI-PEC and Ag@PANI-PEC exhibited biocompatibility and the presence of silver on Ag@PANI-PEC rendered antibacterial properties to the latter, thus making them an ideal material for *in vivo* implants. These findings establish the feasibility of using the nanocomposite as a potential material for energy storage device in IEMDs.

Received 8th May 2014
Accepted 19th May 2014

DOI: 10.1039/c4tb00739e

www.rsc.org/MaterialsB

1. Introduction

Recently, there is a growing need for nanohybrid materials with an unusual combination of properties to satisfy the challenges faced by modern biomedical science.¹ The late 20th century has seen the propagation of active implantable electronic medical devices (IEMDs). IEMDs comprise a broad range of products, which include life-supporting implants like pacemakers, heart valves, cochlear implants, neurostimulators, and defibrillators. The IEMDs are used increasingly to sustain and improve patients' health. The increase in the production of IEMDs has

stimulated an increasing demand for high performance power sources like the supercapacitor. Supercapacitors which store energy by separation of charges have piqued people's curiosity over the past decade due to their high power density, low maintenance cost and long durability.² Generally, they are coupled with fuel cells or batteries to deliver high power in electrical energy storage and harvesting applications. The capacitance in supercapacitor originates either from the charging–discharging of the electrical double layers or from the Faradaic redox reactions. In the former case, the capacitance is derived from the charge separation in carbon-based materials while in the latter, a Faradaic process takes place due to the redox reactions in metal oxides or conducting polymers. The properties required to make a good electrochemical capacitor include good electronic conductivity, chemical stability to alkaline and acidic electrolytes, low cost, and high specific surface area.² In addition to the above characteristics, supercapacitors for *in vivo* application need to function under physiological conditions. The prerequisites to fabricate such devices are (i) to make use of material which is biocompatible with the human body, (ii) to operate and sustain the devices in physiological fluids, and (iii) to make the devices with processable materials. In the case of temporary implantation, the materials which are used for IEMDs can be easily removed after the

^aChemistry Division, Bhabha Atomic Research Centre, Trombay, Mumbai 400085, India. E-mail: stawde@barc.gov.in; Tel: +91 22 25590288

^bDepartment of Biotechnology, Indian Institute of Technology, Chennai, India

† Electronic supplementary information (ESI) available: The details of materials, characterization techniques, PANI-PEC and Ag@PANI-PEC syntheses, electrode preparation and sample preparation for biocompatibility/bacterial adhesion studies are given. Additional experimental findings including the influence of pectin on the nanocomposite yield, energy dispersive X-ray spectroscopy (EDX) data of Ag@PANI-PEC, UV-visible spectral data of PANI-PEC, *in vitro* biocompatibility and antibacterial study of polymer films are also given. A table with sample description, synthesis conditions, values of specific capacitance (C_{sp}), % cell viability (biocompatibility), and bacterial adhesion (antibacterial activity) is given. See DOI: 10.1039/c4tb00739e

purpose is served. However, these implantable medical devices are linked to the ultimate peril of bacterial infection.³ If the system has antibacterial properties, it will be potentially useful for biomedical applications.^{4,5}

In recent decades, there has been a growing interest in the construction of supercapacitor electrodes with conducting polymers, especially PANI, due to its facile synthesis, redox property, tuneable morphology, low cost and better environmental stability as compared to other conducting polymers.⁶ One of the major drawbacks of PANI is its poor solution processability. Processable PANI can be synthesized using sulfonic and dicarboxylic acid dopants.^{6,7} However, the PANI thus obtained is processable only in organic solvents which are not eco-friendly and thus the process is not compatible with biological applications. The preparation of PANI dispersion is one of the ways to overcome this difficulty since colloidal dispersions can often be applied in place of true solutions.^{8,9} Water dispersible PANI can be prepared using many conventional water soluble polymers and biopolymers as stabilizers.^{6,10} The use of biopolymers as a stabilizer not only improves the processability of PANI in water but also imparts biocompatibility for potential biomedical applications.¹¹ Biopolymers have seldom been used with PANI for supercapacitor application due to their insulating and non-electroactive nature which consequently increases the resistance of the electrodes. However, PANI or conducting polymers can be combined with carbon or metal oxides for higher specific capacitance and stability.^{12–14} Morphology of the electrode material also plays a vital role in enhancing specific capacitance.¹⁵ In our previous research, we synthesized PANI nanorods and nanospheres on aniline-primed indium tin oxide substrate and studied their morphology-dependent supercapacitive property, in which nanorods showed a higher specific capacitance than nanospheres due to the availability of larger surface area for redox reactions.^{16,17}

To the best of our knowledge, researchers have used carbon,^{18,19} metal oxides,^{20,21} conducting polymers^{22,23} and their combinations^{24–29} for supercapacitor application in acidic/basic/neutral aqueous or organic electrolytes. Supercapacitors operating in physiological fluids for application in IEMDs have seldom been reported. Recently, Malika and Jan modified PANI with multi-walled carbon nanotubes on a stainless steel substrate and used the resulting modified substrate as a supercapacitor electrode which can operate in physiological fluids.³⁰ Victor *et al.* demonstrated the design, fabrication, and packaging of flexible carbon nanotubes–cellulose-based nanocomposite sheets for energy storage application like supercapacitors, Li-ion batteries, and hybrids³¹ in physiological fluids. However, carbon nanotubes are not suitable for *in vivo* applications due to their potential toxicity.³² Herein, for the first time, we demonstrate the synthesis of a supercapacitor electrode material with an unusual combination of properties such as processability, electroactivity, biocompatibility, antibacterial property and ability to operate in physiological fluids. PANI, a conducting polymer, was modified by PEC, a biopolymer, to obtain water dispersible PANI-PEC, which was further treated with an AgNO₃ solution to form Ag NPs decorated PANI-PEC

(Ag@PANI-PEC). The Ag@PANI-PEC exhibited satisfactory supercapacitive property in physiological fluids like PBS, blood, urine and serum.

2. Experimental section

Water dispersible PANI-PEC was synthesized by the polymerization of aniline at room temperature in the presence of stabilizer PEC at various aniline : PEC w/w ratio (1 : 1, 1 : 2 and 1 : 3 and named as PP11, PP12, and PP13 respectively). Then the PANI-PEC was treated with 0.1 M AgNO₃ solution at 60 °C to afford Ag NPs decorated PANI-PEC (Ag@PANI-PEC) and named as Ag111, Ag121, and Ag131, respectively. To study the effect of AgNO₃ concentration on Ag@PANI-PEC synthesis, PANI-PEC (PP12) was treated with 0.05 M and 0.2 M AgNO₃ solution at 60 °C to afford Ag NPs decorated PANI-PEC which were named as Ag1205 and Ag122 respectively. PANI-PEC itself helped in the reduction of silver ions to form Ag NPs; hence, external reducing agent was not used. The working electrode for electrochemical characterization was prepared by casting a known quantity of PANI-PEC or Ag@PANI-PEC dispersion on glassy carbon electrode (GCE). The details of the synthesis, electrode preparation and characterization are given in ESI.†

3. Results and discussion

3.1 Synthesis of PANI-PEC

Water dispersible PANI-PEC was synthesized using various amounts of biopolymer PEC (1 : 1, 1 : 2 and 1 : 3 w/w of aniline : PEC) as a stabilizer. Table S1 in ESI† shows the yield of the polymerization, amount of PEC present in the PANI-PEC and subsequent particle size with varying amount of PEC in the reaction mixture. The resulting PANI-PEC showed an average particle size of 690 ± 10 nm, 340 ± 10 nm, and 730 ± 10 nm with polydispersity index (PDI) of 0.52 ± 0.05, 0.07 ± 0.02, and 0.59 ± 0.03, respectively, as analyzed by dynamic light scattering (DLS) measurement. The particle size of PANI-PEC was higher in the case of 1 : 1 and 1 : 3 w/w of aniline : PEC due to insufficient and excess coverage of PEC on the PANI particles, respectively, whereas 1 : 2 ratio gives a highly uniform particle size (PDI = 0.07). An insufficient amount of stabilizer PEC can cause macroscopic aggregation because the π–π interaction between PANI particles can overcome the stabilizing capacity of PEC. At the same time, an excess amount of PEC on PANI can form gel-like structure due to water absorption and swelling which consequently increases the particle size of PANI-PEC. This is also reflected in the yield of polymerization as an increase in the amount of PEC in the aniline polymerization increased the yield of polymerization (Table S1†). During the synthesis, the stability of the dispersion and electroactivity of the product should be considered. It is essential to have a reasonable amount of PEC on the surface of the PANI particles to keep the PANI-PEC dispersion stable without aggregation. On the other hand, increases in the amount of stabilizer decreases the electroactivity of the product due to the insulating and non-electroactive nature of the stabilizer. In this situation, the PANI-PEC (PP13) synthesized using 1 : 3 aniline : PEC ratio is not

suitable for electrochemical studies. Keeping this in mind, the PANI-PEC synthesized using 1 : 2 aniline : PEC w/w (PP12) which provided reasonable dispersion stability and electroactivity was considered as an optimum material for further studies. The PANI-PEC dispersion (Fig. 1a) prepared in our laboratory is stable over eight months under normal atmospheric conditions, and we believe that it will be stable for at least one year without any macroscopic precipitation.

3.2 Synthesis of Ag@PANI-PEC

PANI-PEC in water was treated with AgNO_3 solution at 60 °C to afford water dispersible Ag@PANI-PEC. Here, no additional reducing agent was required as PANI-PEC itself acted as a reducing agent to reduce Ag^+ ions to Ag^0 which was adsorbed onto the surface of PANI-PEC. In this experiment, a constant amount (in terms of concentration and volume) of PANI-PEC solution was used and the concentration of AgNO_3 was varied (0.05 M to 0.2 M) to study the reduction effectiveness of PANI-PEC. The concentration of 0.1 M was found to be ideal because, at lower AgNO_3 concentration, there was no significant formation of Ag@PANI-PEC. Ag@PANI-PEC synthesized at higher AgNO_3 concentration was not dispersible in water which could be due to the aggregation of silver and PANI-PEC. In our previous work, PANI was used to reduce Au^+ ions to form PANI-Au nanocomposite which is insoluble in water and organic solvents.³³ Tamboli *et al.* synthesized PANI-Ag NPs using PANI as the reducing agent and studied the antibacterial properties.³⁴ Our research group has earlier carried out biocompatibility studies on PANI-Ag NPs nanocomposite where sodium citrate was used as the reducing agent.³⁵ Ivanova *et al.* synthesized pectin-Ag nanocomposite using pectin as a reducing agent. However, the reduction was carried out in the presence of sodium hydroxide solution.³⁶ In the present work, water dispersible PANI-PEC was used as a reducing agent to convert Ag^+ ions to Ag NPs on PANI-PEC (Fig. 1b). The hydroxyl groups in the PEC can facilitate inter- and intra-molecular hydrogen

bonding to form supramolecular cages which allow the diffusion and reduction of Ag^+ ions in its vicinity.³⁷ In summary, PANI-PEC works as the following: (i) a template for Ag^+ reduction and formation of Ag^0 on its surfaces, (ii) a green reducing agent, (iii) a stabilizer to prevent the Ag^0 from aggregation, and (iv) a stabilizer to afford the dispersibility of Ag@PANI-PEC in water.

3.3 Characterization

3.3.1 Field emission-scanning electron microscopy (FE-SEM) analysis. The FE-SEM image of PANI-PEC (PP12) showed a 'flattened rice' morphology with 150 nm length and 40 nm diameter (Fig. 1c and d). The dimensions obtained from FE-SEM image are much lower as compared to the size obtained from DLS studies (340 nm). DLS measurements give the average hydrodynamic radius of diffusing particles. PEC is known to swell to a large extent in aqueous medium, which can lead to a high hydrodynamic radius for PANI-PEC in dispersion. In the case of Ag@PANI-PEC (Ag121), the continuous growth of Ag NPs on the PANI-PEC shows the transition of flattened rice like morphology to nanocubes with the edge length of about 75 nm (Fig. 1e and f). The EDX (electron dispersive X-ray spectroscopy) analysis indicates the presence of 15% Ag in the particles (ESI Fig. S1†).

3.3.2 X-ray diffraction (XRD) analysis. Fig. 2a shows the XRD pattern of PANI-PEC (inset) and Ag@PANI-PEC. The diffractogram of PANI-PEC displayed two small humps around $2\theta = 20^\circ$ and 25° which indicate the amorphous nature of the PANI-PEC. These are ascribed to periodicity parallel and perpendicular to the polymer chain, respectively.³⁸ The XRD pattern of Ag@PANI-PEC (Fig. 2a) exhibits distinct diffraction peaks at 38.177° , 44.278° , 64.427° , 77.425° , and 81.539° which are indexed to (111), (200), (220), (311) and (222) planes of metallic silver, indicating a crystalline cubic structure (JCPDS file: 65-2871). The formation of Ag NPs on the PANI-PEC surface proves the efficiency of the PANI-PEC as a reducing agent.

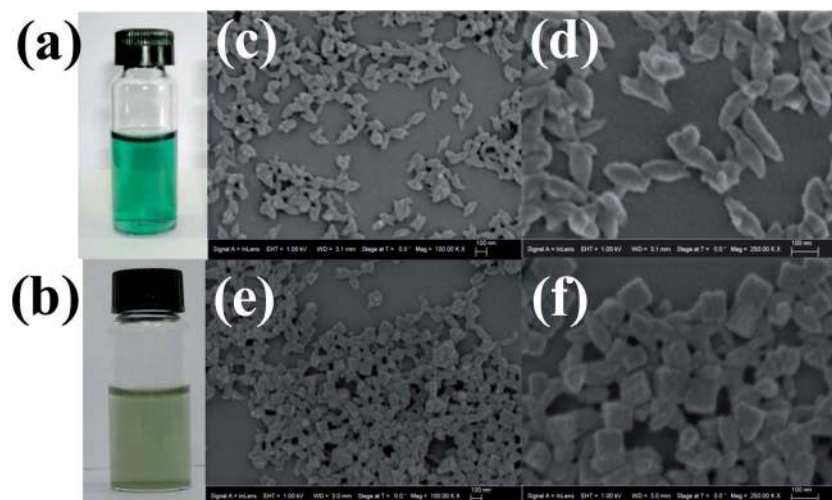


Fig. 1 Photographs of (a) PANI-PEC and (b) Ag@PANI-PEC dispersion in water; FE-SEM images of PANI-PEC (c and d) and Ag@PANI-PEC (e and f).

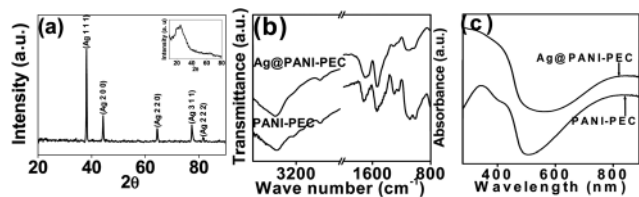


Fig. 2 (a) XRD patterns of Ag@PANI-PEC (Ag121) and PANI-PEC (PP12) (inset); (b) FTIR and; (c) UV-visible spectra of Ag@PANI-PEC (Ag121) and PANI-PEC (PP12).

3.3.3 Fourier transform infrared spectroscopy (FTIR) analysis. The FTIR spectra for PANI-PEC and Ag@PANI-PEC are depicted in Fig. 2b. The spectra are complex and show a considerable broadening when compared to that of conventional PANI¹⁰ which could be due to the various vibrations of PEC, which has a complex polymeric structure. The broad band from 3640 cm^{-1} to 3300 cm^{-1} centred at 3420 cm^{-1} shows an O–H stretching vibration from the PEC. The band at 2930 cm^{-1} is due to the asymmetric stretching of an aliphatic C–H in PEC. The C=O stretching of carbonyl group of PEC and C=C stretching of quinoid rings of PANI merge together to give a broad peak centred at 1695 cm^{-1} . The peaks at 1540 cm^{-1} and 1300 cm^{-1} show the presence of C=C stretching vibration of benzenoid rings and C–N stretching in the PANI, respectively. The peak related to the N=C=N bending vibration of PANI is shifted to a lower wave number of 1110 cm^{-1} from 1125 cm^{-1} , which was possibly caused by the hydrogen bonding between PEC and imine group of the PANI chains.³⁹

3.3.4 UV-visible spectroscopy analysis. UV-visible spectrum of green colored PANI-PEC (Fig. 2c) displayed three peaks at around 330 nm (π – π^* transition in the benzenoid ring of PANI system), 430 nm (polaron to π^* transition in doped form of PANI) and 870 nm (π to polaron transition, signature of doped form of PANI system) which originate from the electronic transitions characteristic of semi-oxidized protonated form of PANI.¹⁰ The Table S2 (ESI)[†] shows the UV-visible spectroscopy data of PANI dispersion which are prepared using 1 : 1, 1 : 2, 1 : 3 aniline : PEC w/w. The increasing amount of PEC stabilizer did not influence the PANI peak positions. The observations of bands in UV-visible spectra of PANI-PEC prove its dispersibility in water. The PEC on the surface of PANI forms hydrogen-bonding with water which leads to a higher degree of dispersibility of PANI-PEC.

UV-visible absorption spectrum of Ag@PANI-PEC is shown in Fig. 2c. Surface plasmon resonance is a vital optical property of nanoparticles and is illustrated as coherent fluctuations in electron density occurring at the ‘free electron’ metal–dielectric interface. It is well-known that colloidal Ag NPs exhibit absorption at wavelengths from 390 to 420 nm due to Mie scattering. Generally, the polaron to π^* transition peak of the PANI system is also observed in this range (420 – 430 nm). The surface plasmon resonance peak of Ag and polaron to π^* transition peak of PANI were found to overlap, leading to a broad band in the 300 to 400 nm region in the case of Ag@PANI-PEC.⁴⁰

3.3.5 X-ray photoelectron spectroscopy (XPS) analysis. N 1s XPS spectra of PANI-PEC and Ag@PANI-PEC are shown in Fig. 3.

Generally, N 1s XPS spectra of the PANI salt can be deconvoluted into three discrete peaks at 398.2 eV , 399 eV , and 400 eV , which are associated with the quinoid imine, the benzenoid amine and the positively charged nitrogen, respectively.⁴¹ In the present study, both PANI-PEC and Ag@PANI-PEC displayed the three deconvoluted curves in the N 1s region which indicates the presence of PANI in the protonated salt form. The N 1s deconvoluted peak positions of PANI-PEC (399.0 , 400.5 and 401.6 eV) and Ag@PANI-PEC (397.8 , 398.6 and 399.6 eV) are slightly different from that of conventional PANI salt which could be due to the presence of PEC and Ag NPs in its system. The $-\text{NH}/-\text{N}=\text{}$ ratio of PANI-PEC is close to unity whereas for Ag@PANI-PEC the ratio is 0.2 . This shows that the Ag@PANI-PEC contains more oxidized units ($-\text{N}=\text{}$) than the PANI-PEC which could be due to the oxidation of PANI by AgNO_3 which gets reduced to Ag NPs. The peak intensity of the positively charged nitrogen ($-\text{NH}^+$) in Ag@PANI-PEC is higher compared to the PANI-PEC.⁴⁰ The 3d Ag XPS spectrum of Ag@PANI-PEC is shown in Fig. 3. The Ag species of Ag@PANI-PEC display two bands at around 368.3 and 374.2 eV , which can be individually ascribed to Ag $3d_{5/2}$ and Ag $3d_{3/2}$ binding energies.⁴²

3.3.6 Electrochemical studies. In order to evaluate the feasibility of using Ag@PANI-PEC in IEMDs, its supercapacitive property was studied in physiological fluids. Fig. 4a depicts the cyclic voltammograms (CVs) of PANI-PEC, Ag@PANI-PEC, PEC, and bare GCE in PBS electrolyte at a scan rate of 100 mV s^{-1} . PANI-PEC did not display significant electroactivity probably due to the insulating nature of PEC. The CV of Ag@PANI-PEC showed a higher current as compared to PANI-PEC which reflects a better electroactivity despite the presence of PEC as evidenced from the FTIR studies. The presence of Ag NPs helped to expedite electron transport by acting as a bridge between the GCE – PANI and PANI–electrolyte interfaces resulting in

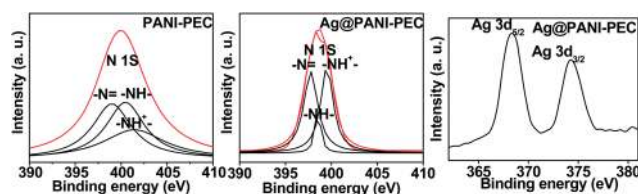


Fig. 3 N 1s XPS spectra of PANI-PEC (PP12) and Ag@PANI-PEC (Ag121); Ag 3d XPS spectra of Ag@PANI-PEC (Ag121).

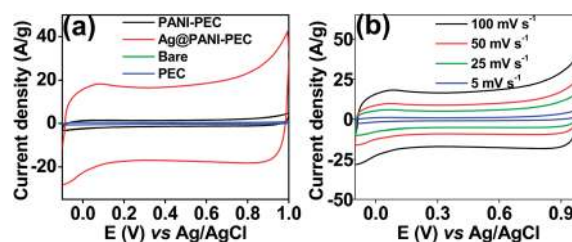


Fig. 4 CVs in PBS from -0.1 to 1.0 V vs. Ag/AgCl of (a) PANI-PEC (PP12), Ag@PANI-PEC (Ag121), bare-GCE and PEC at 100 mV s^{-1} ; (b) Ag@PANI-PEC (Ag121) at scan rates of 100 , 50 , 25 , 5 mV s^{-1} .

reasonable electroactivity in PBS.⁴³ Fig. 4b shows the CV of Ag@PANI-PEC at different scan rates (100, 50, 25, 5 mV s^{-1}) for the potential window of -0.1 to 1.0 V vs. Ag/AgCl in PBS electrolyte. Rectangular shaped CV was obtained demonstrating good charge propagation in the electrodes. It can be seen that the CVs retained their shape even at a high scan rate, indicating that the Ag@PANI-PEC has a rapid current response upon voltage reversal. Even though PANI systems are recognized to display a high pseudo-capacitance due to the existence of numerous oxidation states, Fig. 4 did not show the pseudo-capacitance behavior which might be due to the low proton concentration in the PBS electrolyte. The supercapacitive property of PANI-PEC and Ag@PANI-PEC electrodes in physiological fluids was assessed by conducting galvanostatic charge–discharge measurement at a constant current density of 1.5 A g^{-1} in the potential range between 0 and 0.9 V vs. Ag/AgCl. The specific capacitance (C_{sp}) was calculated from the discharge curve according to the equation $C_{\text{sp}} = i/(m(\Delta V/\Delta t))$, where ‘ m ’ is mass of the active material in grams, ‘ i ’ the applied current in amperes, and $\Delta V/\Delta t$ the slope of the discharge curve.⁴⁴ Based on the equation above, the specific capacitance of PANI-PEC synthesized using 1 : 1, 1 : 2, 1 : 3 aniline : PEC w/w ratio was 25, 15 and 10 F g^{-1} respectively in the PBS electrolyte at the current density of 1.5 A g^{-1} . Consequently, the specific capacitance of Ag nanocomposites (Ag@PANI-PEC) which was prepared using PANI-PEC samples above in PBS electrolyte at the current density of 1.5 A g^{-1} was 40, 140, and 37.5 F g^{-1} respectively. A representative plot for the charge–discharge curve of PANI-PEC (synthesized using 1 : 2 aniline : PEC w/w ratio) and Ag@PANI-PEC (prepared using PANI-PEC which was synthesized using 1 : 2 aniline : PEC w/w ratio and 0.1 M AgNO_3 and named as Ag121) is shown in Fig. 5a. To understand the influence of the amount of Ag NPs on the specific capacitance, Ag@PANI-PEC was synthesized using different molar concentrations of AgNO_3 (0.05 M and 0.2 M , named as Ag1205 and Ag122 respectively). Galvanostatic charge–discharge studies for Ag1205 and Ag122 gave a specific capacitance of 25 and 135 F g^{-1} respectively (Fig. 5b). The lesser specific capacitance of Ag1205 could be due to the presence of insufficient amount of Ag NPs on the PANI-PEC. Charge–discharge cycle stability is another important property for supercapacitor electrode material. The normalized capacitance (%) of Ag@PANI-PEC in PBS as a function of cycle number (current density of 2.5 A g^{-1}) is

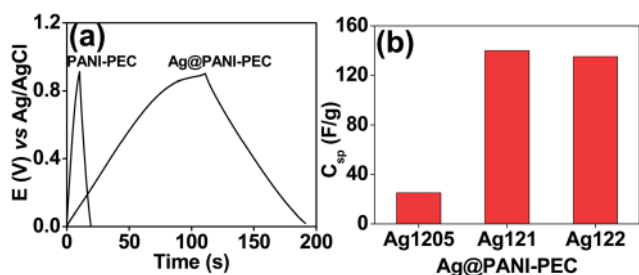


Fig. 5 (a) Galvanostatic charge–discharge curves of PANI-PEC (PP12) and Ag@PANI-PEC (Ag121) and (b) C_{sp} of Ag@PANI-PEC which was prepared using different molar concentrations of AgNO_3 .

depicted in Fig. S2a (ESI).[†] The capacitance of the Ag@PANI-PEC was found to decrease sharply over 250 charge–discharge cycles while retaining 80% of the initial value. After this, there was only 12% loss from 250 to 1000 cycles while retaining 68% of the initial capacitance (Fig. S2a[†]). PANI is known to lose its electroactivity to a certain extent on continuous cycling, especially in solutions with high pH.⁴⁵ Nonetheless, Ag@PANI-PEC exhibited satisfactory electroactivity and specific capacitance even after 1000 cycles due to the presence of Ag NPs. The stability can be further improved by operating the electrode in a lower voltage range to avoid oxidation and decomposition of polyaniline. Hence, galvanostatic charge–discharge was carried out at 2.5 A g^{-1} in the lower voltage range of 0 – 0.6 V vs. Ag/AgCl. In this case, there was only a 5% loss over 250 cycles and at the end of 1000 cycles, 85% of the initial capacitance was retained (Fig. S2b[†]). Thus, depending on the type of application, the voltage range can be tuned to get the desired capacitance and stability. In view of results above, the Ag@PANI-PEC (prepared by PANI-PEC synthesized using 1 : 2 aniline : PEC w/w ratio and 0.1 M AgNO_3), with a reasonable specific capacitance of 140 F g^{-1} , was chosen for further studies in other physiological fluids like blood, urine and serum.

Fig. 6a shows the CV of Ag@PANI-PEC in PBS, blood, urine and serum supporting electrolytes at the scan rate 100 mV s^{-1} for the potential window of -0.1 V to 1.0 V vs. Ag/AgCl. As compared to PBS, the nature of CV in these electrolytes was found to be different due to the presence of complex components in these physiological fluids. Consequently, the specific capacitance of Ag@PANI-PEC in blood, urine, and serum at the current density of 1.5 A g^{-1} was found to be 290, 144, and 121 F g^{-1} respectively (Fig. 6b). The potential vs. time plot in the charge–discharge experiment (Fig. 6b) is not an ideal ‘inverted V’ shaped curve (linear and typical triangular distribution) as expected in the case of electrical double layer capacitance. Generally, in the case of a pseudo-capacitance, a slightly distorted ‘inverted V’ shape curve is observed due to the Faradaic processes involved. The distortion in PBS, urine and serum are not that significant as compared to that of blood, probably due to the complex composition of the latter.

Based on the electrochemical investigations, it can be summarized that Ag@PANI-PEC display reasonable specific

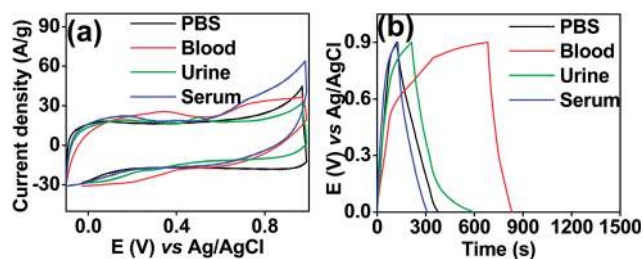


Fig. 6 (a) CVs of Ag@PANI-PEC (Ag121) from -0.1 to 1.0 V vs. Ag/AgCl in PBS, blood, urine and serum at the scan rate of 100 mV s^{-1} ; (b) charge–discharge curve of Ag@PANI-PEC (Ag121) in PBS, blood, urine and serum at the cut off voltage from 0 to 0.9 V vs. Ag/AgCl.

capacitance in physiological fluids due to the synergistic effect of its components: PANI and Ag NPs. The nano-sized morphology of Ag@PANI-PEC expedites ion diffusion from the electrolytes to the electrode, making full utilization of the active materials. Moreover, the Ag NPs present on the surface of Ag@PANI-PEC facilitates quick electron transfer from the electrode to electrolytes by the bridging effect. The PEC present in Ag@PANI-PEC electrode could form supramolecular assemblies or nanocages on the surface of the electrode by inter- and intra-molecular hydrogen-bonding. These nanocages trap the electrolytes near the electrode surface and increase the interactions between the electrode and electrolytes, and hence, provide a high specific capacitance to the material despite its insulating and non-electroactive nature. The nanocages on the surface also prevent the electrode material from shrinking during the intercalation/de-intercalation of the counter ions.^{46,47} These studies revealed that the electroactivity of Ag@PANI-PEC in physiological fluids can be utilized for potential applications in IEMDs.

Generally, supercapacitor for IEMDs is less likely to come in direct contact with the tissue or blood as it will be packed well inside the device casing. However, in the case of casing malfunction, there is a probability of the supercapacitor material being exposed to the tissue/blood. From this point of view, biocompatibility and antibacterial studies were carried out to analyze the safety of the material.

3.3.7 *In vitro* biocompatibility of polymer films. The biocompatibility of polymer films was assessed with L6 rat myoblast cells and the cell viability was determined by MTT assay.⁴⁸ The percentage of viable cells was 83.16, 89.28, and 91.01% for PANI-PEC (Fig. S3a in ESI[†]) prepared using 1 : 1, 1 : 2, 1 : 3 aniline : PEC w/w. The viability of the cells increased as the amount of PEC increased in the PANI-PEC. This is because PEC is a biopolymer and well established for its biocompatibility. On the other hand, the % cell viability of respective Ag NPs decorated PANI-PEC nanoparticles was 94.41, 89.77, and 77.35% (Fig. S3b in ESI[†]). Pectin acts as a mild reducing agent and favors the formation of Ag NPs.³⁶ It is reported that silver-PEC nanoparticles enhance the singlet oxygen production by 1.8 fold and induce selective damage to the tissues.⁴⁹ Higher concentration of PEC in our case could lead to a higher formation of Ag NPs thus reducing the cell viability. When the concentration of AgNO₃ solution was varied (0.2 M, 0.1 M and 0.05 M), the resulting Ag@PANI-PEC exhibited 44.67, 89.77 and 87.18% cell viability, respectively (Fig. S3c in ESI[†]). There are several reports in literature on the cytotoxicity associated with silver nanoparticles due to the presence of unconverted Ag⁺ ions which are known to be toxic to the cells.⁵⁰ Hence, in the present work, the samples were washed with 1% ammonia solution to remove AgCl which resulted in improved biocompatibility. Based on these studies, it could be concluded that 0.1 M AgNO₃ is the optimum concentration required to afford nanocomposite with reasonable cell viability.

3.3.8 Bacterial adhesion assay. Adhesion of Gram negative *Escherichia coli* (NCIM 2931) was tested on polymer films.⁴⁸ The values of bacterial adhesion for various samples of PANI-PEC

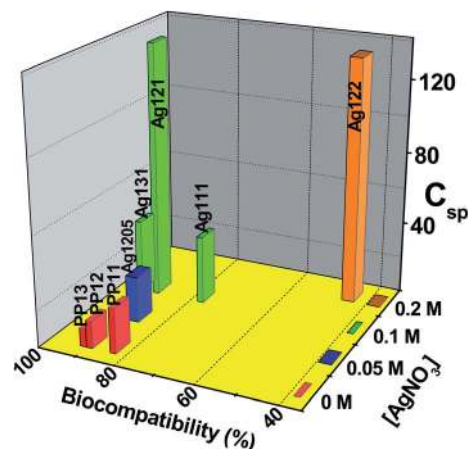


Fig. 7 Specific capacitance (F g⁻¹) and biocompatibility for various PANI-PEC and Ag@PANI-PEC samples. [Abbreviations: PP11, PP12 and PP13 = PANI-PEC synthesized using different ratio of aniline : PEC w/w, (1 : 1, 1 : 2 and 1 : 3, respectively); Ag111, Ag121, Ag131 = Ag@PANI-PEC synthesized from PP11, PP12 and PP13 using 0.1 M AgNO₃; and Ag1205, Ag121, Ag122 = Ag@PANI-PEC synthesized from PP12 using different concentrations of AgNO₃ (0.05 M, 0.1 M and 0.2 M, respectively)].

and Ag@PANI-PEC are shown in Table S3 in ESI[†]. The bacterial adhesion was found to increase with the amount of PEC but decreased drastically with the increase in the amount of Ag NPs, which could be attributed to the antibacterial property endowed by Ag NPs (Fig. S4 in ESI[†]). Here too, it was observed that the Ag@PANI-PEC prepared using 0.1 M AgNO₃ and PANI-PEC (synthesized using 1 : 2 w/w aniline : PEC) gave the optimum antibacterial property. The results above reveal that the biocompatible and antibacterial nature of PANI-PEC and Ag@PANI-PEC can be tuned according to the composition (and as per the application), and this increases the feasibility of using these materials for *in vivo* applications.

In the present work, four properties namely, (a) electroactivity or specific capacitance in physiological fluids, (b) biocompatibility, (c) antibacterial activity and (d) water dispersibility have been introduced in a single nanocomposite. The results of this study (Fig. 7, S5 and Table S3 in ESI[†]) can help to select an appropriate composition based on the envisaged application. Improving one property of the nanocomposite could affect another property; hence, an appropriate composite should be selected based on the requirements. Our research group is working on silver nanocomposites to further improve the electroactivity, biocompatibility and water dispersibility simultaneously.

4. Conclusions

To conclude, we demonstrate the synthesis of water dispersible nanocomposite Ag@PANI-PEC exhibiting electroactivity, specific capacitance (in physiological fluids) as well as reasonable biocompatibility and antibacterial properties. The specific capacitance of Ag@PANI-PEC at the current density 1.5 A g⁻¹ was 140, 290, 144, and 121 F g⁻¹ in PBS, blood, urine, and

serum, respectively. These results support that this nanocomposite may have commercial potential for environmentally friendly and inexpensive supercapacitor electrode in biomedical applications. Furthermore, the biocompatibility and antibacterial nature of the Ag@PANI-PEC endorse the feasibility of using it for *in vivo* applications. Forthcoming effort will be emphasized on additional characterizations, review of the mechanism, and trials of *in vivo* implantation. The enhancement of the electroactivity and biocompatibility of the nanocomposite is currently underway.

Acknowledgements

CAA is grateful to BRNS, Department of Atomic Energy, for providing KSKRA fellowship. Authors are thankful to Dr C. B. Basak and Dr M. Krishnan (for FE-SEM measurements), Dr Jagannath (for XPS measurements), Mr J. Nuwad (for EDX measurement), and Ms J. A. Prabhu and Mr S. D. Kamble (for providing blood, urine, and serum samples) from BARC for their support during this work.

Notes and references

- C. A. Amarnath, S. S. Nanda, G. C. Papaefthymiou, D. K. Yi and U. Paik, *Crit. Rev. Solid State Mater. Sci.*, 2013, **38**, 1.
- A. Burke, *J. Power Sources*, 2000, **91**, 37.
- M. Jamal, F. M. Shaikh, B. Aslam and K. M. Razeeb, *Anal. Methods*, 2012, **4**, 1865.
- I. Mahapatra, J. Clark, P. J. Dobson, R. Owen and J. R. Lead, *Environ. Sci.: Processes Impacts*, 2013, **15**, 123.
- M. C. C. Ferrer, N. J. Hickok, D. M. Eckmann and R. J. Composto, *Soft Matter*, 2012, **8**, 2423.
- S. Bhadra, D. Khastgir, N. K. Singha and J. H. Lee, *Prog. Polym. Sci.*, 2009, **34**, 783.
- S. Palaniappan and C. A. Amarnath, *React. Funct. Polym.*, 2006, **66**, 1741.
- M. Aldissi, *Adv. Mater.*, 1993, **5**, 60.
- S. P. Armes and M. Aldissi, *J. Chem. Soc., Chem. Commun.*, 1989, 88.
- C. A. Amarnath, S. Palaniappan, P. Rannou and A. Pron, *Thin Solid Films*, 2008, **516**, 2928.
- M. Li, Y. Guo, Y. Wei, A. G. MacDiarmid and P. I. Lelkes, *Biomaterials*, 2006, **27**, 2705.
- Z. Niu, P. Luan, Q. Shao, H. Dong, J. Li, J. Chen, D. Zhao, L. Cai, W. Zhou, X. Chen and S. Xie, *Energy Environ. Sci.*, 2012, **5**, 8726.
- W. Wang, Q. Hao, W. Lei, X. Xia and X. Wang, *RSC Adv.*, 2012, **2**, 10268.
- M. Sawangphruk, M. Suksomboon, K. Kongsupornsak, J. Khuntilo, P. Srimuk, Y. Sanguansak, P. Klunbud, P. Suktha and P. Chiochan, *J. Mater. Chem. A*, 2013, **1**, 9630.
- G. A. Snook, P. Kao and A. S. Best, *J. Power Sources*, 2011, **196**, 1.
- C. A. Amarnath, J. H. Chang, D. Y. Kim, R. S. Mane, S. H. Han and D. Sohn, *Mater. Chem. Phys.*, 2009, **113**, 14.
- C. A. Amarnath, J. H. Chang, J. Lee, D. Y. Kim, R. S. Mane, S. H. Han and D. Sohn, *Electrochem. Solid-State Lett.*, 2008, **11**, A167.
- F. Zhang, T. Zhang, X. Yang, L. Zhang, K. Leng, Y. Huang and Y. Chen, *Energy Environ. Sci.*, 2013, **6**, 1623.
- L. L. Zhang, R. Zhou and X. S. Zhao, *J. Mater. Chem.*, 2010, **20**, 5983.
- X. Zhang, D. Zhao, Y. Zhao, P. Tang, Y. Shen, C. Xu, H. Li and Y. Xiao, *J. Mater. Chem. A*, 2013, **1**, 3706.
- X. Wang, A. Sumboja, M. Lin, J. Yan and P. S. Lee, *Nanoscale*, 2012, **4**, 7266.
- G. A. Snook, T. L. Greaves and A. S. Best, *J. Mater. Chem.*, 2011, **21**, 7622.
- S. Chen, W. Xing, J. Duan, X. Hu and S. Z. Qiao, *J. Mater. Chem. A*, 2013, **1**, 2941.
- M. Zhi, C. Xiang, J. Li, M. Li and N. Wu, *Nanoscale*, 2013, **15**, 72.
- S. Boukhalifa, K. Evanoff and G. Yushin, *Energy Environ. Sci.*, 2012, **5**, 6872.
- W. Li, X. Yan, J. Chen, Y. Feng and Q. Xue, *Nanoscale*, 2013, **5**, 6053.
- K. Wang, P. Zhao, X. Zhou, H. Wu and Z. Wei, *J. Mater. Chem.*, 2011, **21**, 16373.
- J. Dev, R. I. Jafri, A. K. Mishra and S. Ramaprabhu, *J. Mater. Chem.*, 2011, **21**, 17601.
- J. Duay, E. Gillette, R. Liu and S. B. Lee, *Phys. Chem. Chem. Phys.*, 2012, **14**, 3329.
- M. Ammam and J. Fransaer, *Chem. Commun.*, 2012, **48**, 2036.
- V. L. Pushparaj, M. M. Shaijumon, A. Kumar, S. Murugesan, L. Ci, R. Vajtai, R. J. Linhardt, O. Nalamasu and P. M. Ajayan, *Proc. Natl. Acad. Sci. U. S. A.*, 2007, **104**, 13574.
- Y. Liu, Y. Zhao, B. Sun and C. Chen, *Acc. Chem. Res.*, 2013, **46**, 702.
- M. Rohwerder, S. I. Uppenkamp and C. A. Amarnath, *Electrochim. Acta*, 2011, **56**, 1889.
- M. S. Tamboli, M. V. Kulkarni, R. H. Patil, W. N. Gade, S. C. Navale and B. B. Kale, *Colloids Surf., B*, 2012, **92**, 35.
- P. K. Prabhakar, S. Raj, P. R. Anuradha, S. N. Sawant and M. Doble, *Colloids Surf., B*, 2011, **86**, 146.
- N. V. Ivanova, N. N. Trofimova, L. A. Es'kova and V. A. Babkin, *Int. J. Carbohydr. Chem.*, 2012, **2012**, 459410, 9 pages.
- E. Bulut and M. Özacar, *Ind. Eng. Chem. Res.*, 2009, **48**, 5686.
- C. A. Amarnath, J. Kim, K. Kim, J. Choi and D. Sohn, *Polymer*, 2008, **49**, 432.
- A. Tiwari and V. Singh, *Carbohydr. Polym.*, 2008, **74**, 427.
- C. M. Correa, R. Faez, M. A. Bizeto and F. F. Camilo, *RSC Adv.*, 2012, **2**, 3088.
- E. T. Kang, K. G. Neoh and K. L. Tan, *Prog. Polym. Sci.*, 1998, **23**, 277.
- R. Ji, W. Sun and Y. Chu, *RSC Adv.*, 2014, **4**, 6055.
- K. S. Kim and S. J. Park, *Synth. Met.*, 2012, **162**, 2107.
- H. P. Cong, X. C. Ren, P. Wang and S. H. Yu, *Energy Environ. Sci.*, 2013, **6**, 1185.
- S. Tawde, D. Mukesh and J. V. Yakhmi, *Synth. Met.*, 2002, **125**, 401.

- 46 J. Xu, K. Wang, S. Z. Zu, B. H. Han and Z. Wei, *ACS Nano*, 2010, **4**, 5019.
- 47 J. Zhang and X. S. Zhao, *J. Phys. Chem. C*, 2012, **116**, 5420.
- 48 V. Nandakumar, G. Suresh, S. Chittaranjan and M. Doble, *Ind. Eng. Chem. Res.*, 2013, **52**, 751.
- 49 L. S. A. de Melo, A. S. L. Gomes, S. Saska, K. Nigoghossian, Y. Messaddeq, S. J. L. Ribeiro and R. E. J. de Araujo, *J. Fluoresc.*, 2012, **22**, 1633.
- 50 S. Zhang, C. Du, Z. Wang, X. Han, K. Zhang and L. Liu, *Toxicol. in Vitro*, 2013, **27**, 739.